Optical Engineering

SPIEDigitalLibrary.org/oe

Design of a spiral silica photonic crystal fiber for nonlinear applications in visible region

Md. Nazmul Hossain
M. Shah Alam
Dihan Md. Nuruddin Hasan
K. M. Mohsin

SPIE

Design of a spiral silica photonic crystal fiber for nonlinear applications in visible region

Md. Nazmul Hossain, M. Shah Alam, Dihan Md. Nuruddin Hasan, and K. M. Mohsin
Bangladesh University of Engineering and Technology, Department of Electrical and Electronic Engineering, Dhaka 1000, Bangladesh
E-mail: shalam@eee.buet.ac.bd

Abstract. A silica spiral photonic crystal fiber is presented here for tailoring two zero dispersion wavelengths (ZDWs) in the visible region. The proposed fiber has two ZDWs (523.1 and 716.8 nm) along with a very high nonlinearity parameter (1060 W^{-1} km^{-1} at 500 nm) around the visible region. The proposed design shows improvement over the group dispersion control and air holes collapsibility of highly air filled hexagonal photonic crystal fiber (HPCF), and low damage threshold of the soft glass photonic crystal fiber. Besides, the low air filling fraction (≈43%) of the proposed design reduces the probability of sustaining higher order modes in the fiber and also ensures easy fabrication due to fewer air holes.
[DOI: 10.1117/1.3600765]

Subject terms: silica spiral photonic crystal fiber; supercontinuum generation; ultraflattened dispersion; finite element method.

Paper 110168LRR received Feb. 19, 2011; revised manuscript received May 26, 2011; accepted for publication May 27, 2011; published online Jul. 6, 2011.

1 Introduction

The supercontinuum generation (SCG) by using microstructured photonic crystal fiber (PCF) has become a topic of intense research since it was reported by Ranka et al.[1] In SCG, tailoring the dispersion to achieve flat, anomalous dispersion with small slope and a zero crossing near/at the pump wavelength is an extremely important aspect.[2] Pumping near a zero dispersion wavelength (ZDW) with higher nonlinearity not only reduces its power requirement but also smoothes the generated supercontinuum power spectra.[3] Therefore, the researchers are working on hexagonal, octagonal and various irregular design architectures towards highly nonlinear dispersion flattened PCF.[4] It has already been reported that silica PCF with asymmetrical hole distribution provides the maximum possible nonlinearity parameter, whereas a very small improvement over the symmetric case may be obtained.[5] A soft glass equiangular spiral PCF has already been reported to be a suitable candidate for SCG pumped at near infrared wavelength of 1064 nm due to its higher nonlinearity parameter (≈5250 $W^{-1}km^{-1}$).[6] Silica is a superior material in the visible region due to its few orders of magnitude higher damage threshold than many other nonlinear materials.[7,8] Therefore, in this work, we have engineered the silica spiral photonic crystal fiber (ES-PCF) design architecture[6] in silica material to achieve ultraflattened zero crossing dispersion curve with higher nonlinearity parameter ($\gamma = 2*\mathrm{Pi}*n_2/\lambda A_{\mathrm{eff}}$) in the visible region. The hexagonal photonic crystal fiber (HPCF) structure is also studied with a view to getting the same dispersion curve as that of the proposed ES-PCF. Then, HPCF and ES-PCF are compared with respect to their air filling fraction (AFF). The simulation for the structure shows an ultrahigh nonlinearity parameter (1060 W^{-1} km^{-1} at 500 nm), and two ZDWs at 523.1 and 717.8 nm in the visible region. So, the proposed PCF may be a suitable candidate for SCG in visible region.

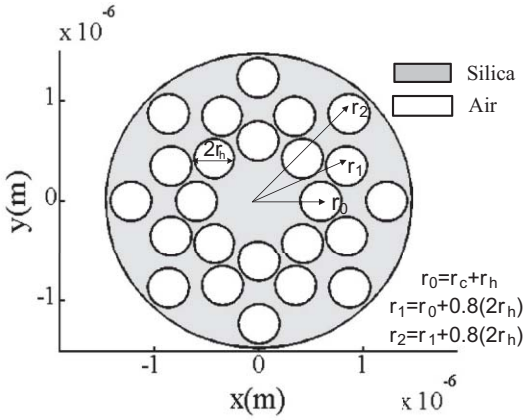

Fig. 1 Cross-section of the spiral PCF.

2 Spiral PCF

Figure 1 shows the cross sectional view of the proposed ES-PCF designed in this work. The proposed fiber material is silica and the cladding air hole distribution is composed of eight spiral arms, each containing three air holes. The first hole in each spiral arm is considered at a distance, $r_0 = r_c + r_h$ from the center where r_c and r_h are assumed as the radius of the core and air hole, respectively. The distance of the second air hole of each arm from the center is $r_1 = r_0 + 0.8(2r_h)$ with an angular displacement of $\theta_1 = 360°/(2N)$, where N is the number of arms. Thus, the n'th air hole in each arm is at a distance of $r_n = r_{n\text{-}1} + 0.8\times(2r_h)$ with an angular displacement of $\theta_n = (n\times 360°)/(2\times N)$ from the first one. Therefore, the first, second, and third hole of each arm constitute the first, second, and third ring, respectively. For the cross section shown in Fig. 1, $r_0 = 0.54$ μm and $r_h = 0.1765$ μm.

In HPCF, tailoring both first and second ZDWs around the visible region will only be possible for a high value of AFF (above 90%),[9] whereas the proposed silica ES-PCF requires only 43% of AFF to do that. The ES-PCF with its low AFF (43%) will help reduce the higher order modes and the probability of collapsing air holes in time of fabricating in such small submicrometer dimensions. Besides, the least total number of air holes of equal size will make its fabrication easier and more precise than that of the conventional HPCF. The proposed PCF may be fabricated by using the sol-gel technique which has already been used for fabricating PCF of various irregular structures.[10]

3 Simulation Results and Discussion

A full-vector FEM[11] has been used to characterize the PCF design. It is known that tapering of a PCF has an

0091-3286/2011/$25.00 © 2011 SPIE

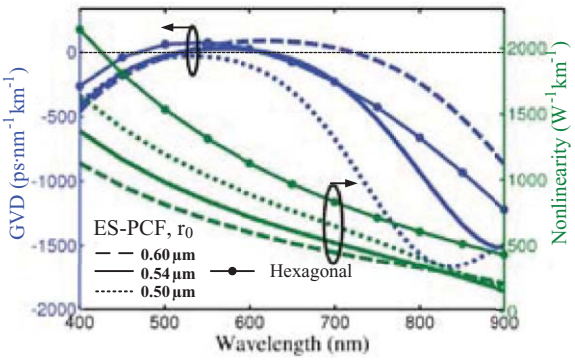

Fig. 2 Dispersion and nonlinearity versus wavelength as a function of core radius.

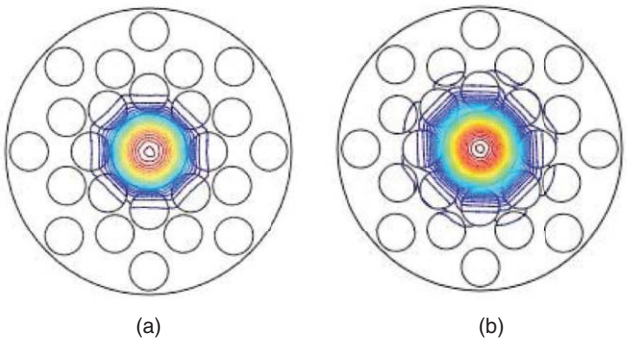

Fig. 3 Electric field over the cross section at (a) 400 nm and (b) 600 nm wavelengths.

important impact on both tailoring the group velocity dispersion (GVD) and increasing nonlinearity.[12] Tailoring the GVD to achieve flat, anomalous dispersion with a small slope and a zero crossing near or at the pump wavelength is an extremely important aspect in SCG. For obtaining nearly zero ultraflattened dispersion in the middle of the visible region, the tapering in and out effects of the proposed geometry is studied.

The GVD and the nonlinearity parameter of ES-PCF as a function of the radius of the core and those of the HPCF are shown in Fig. 2. The Sellmeier equation has been used to find out the refractive index of the fiber material silica at a specific wavelength, and thus the material dispersion has been taken into account. The more the fiber is tapered in, the faster the GVD curve bends down, and shows a higher nonlinearity due to its small effective area. But, due to tapering, the wavelengths far beyond the visible region are less confined in the fiber. Thus, we have optimized the proposed fiber dimension with core diameter 1.08 μm, cladding diameter 2.641 μm, and air hole diameter 0.353 μm, to obtain both higher nonlinearity parameter and nearly zero dispersion in the visible region. It can be seen in Fig. 2 that almost the same pattern of dispersion can be obtained with HPCF with a cost of high value of AFF. For the HPCF (when $\Lambda = 0.55$ μm and $d/\Lambda = 0.97$) with very high AFF (97%) also yields ZDW in the visible region that is comparable with the silica ES-PCF of low AFF (43%). It has been found that for both the structures, the second ZDW exists at 615 nm. But, the nonlinearity of the HPCF is larger than the ES-PCF over the region of wavelength considered here. The high value of AFF (when $d/\Lambda = 0.97$) of the HPCF in such a small dimension ($\Lambda = 0.55$ μm) is not favorable in the fabrication technique due to the high possibility of collapsing air holes in the time of drawing of the fiber.

However, since the soliton self-frequency shift (SSFS) is more efficient in fibers with two ZDWs, a shorter piece of the proposed ES-PCF can be used toward SCG.[3] It is to be mentioned that the proposed ES-PCF shows both the ZDWs (523.1 and 716.8 nm) in the visible region when $r_c = 600$ nm. To our knowledge, attributing both ZDWs in the visible region was not reported before.

To interpret the GVD curve, the contour plot of electric field distribution over the PCF cross section shown in Fig. 3 can be used. At lower wavelengths (below 500 nm), the field is fully confined in the core and interacts solely with the material shown in Fig. 3(a). Therefore, at lower wavelengths dispersion is totally dominated by the material dispersion. The GVD curve remains almost the same before the first ZDW even though the core size varies. As shown in Fig. 3(b), as the wavelength increases, field interacts with the first ring of air holes and waveguide dispersion starts increasing. Afterwards, waveguide dispersion nullifies the material dispersion and yields first ZDW. For further increase in wavelength, the material dispersion starts dominating again while the field interacts with the upper portion of the first air hole ring and finds more silica material in between the two successive holes of the second ring. Therefore, the increasing pattern of dispersion is turned into a flat portion and then curved down, being dominated by the material dispersion. However, the smaller the core size, the higher the nonlinearity parameter due to its small effective area. But, excessive reduction of the core size lowers its GVD curve to a normal dispersion region without any ZDW. As the core size increases, the GVD curve is raised and gives larger bandwidth of anomalous dispersion, whereas, the nonlinearity per unit length decreases.

Figure 4 shows that for both the HPCF and ES-PCF, the nonlinearity parameter decreases as the wavelength increases due to less confinement of light in the core. The higher the confinement in the core, the lower is the value of the effective area, and hence the higher the nonlinearity. The results of Fig. 4 show that the nonlinearity (2142 W^{-1} km^{-1}) in HPCF

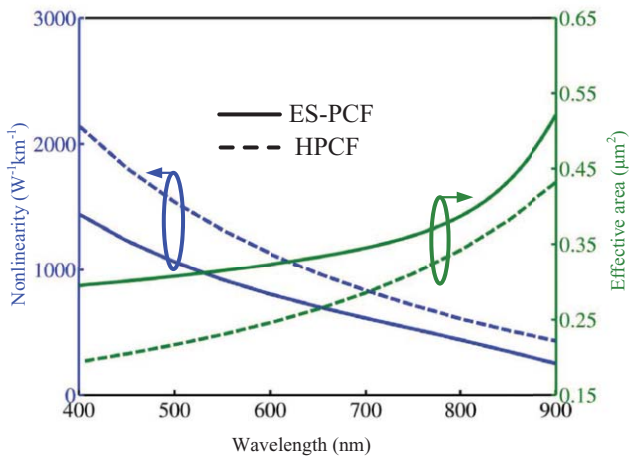

Fig. 4 Nonlinearity and effective area of optimized spiral and hexagonal PCFs.

is larger than that of ES-PCF (1441 W^{-1} km^{-1}), only due to its much smaller core diameter ($\approx$0.52 μm) than the core diameter of the ES-PCF ($\approx$1.08 μm) at a wavelength of 400 nm. However, the results of silica ES-PCF show very high confinement of light (93.43% of total power) in the core with a diameter of 1.08 μm at 500 nm, and thus the overall loss in ES-PCF will be greatly reduced.

4 Conclusion

The proposed silica ES-PCF design has tailored the two ZDWs toward the visible region along with an ultraflattened dispersion curve and high nonlinearity parameter for SCG. Due to low threshold damage in soft glass, Schott SF6, and Tellurite PCFs for long pump pulses (ns) in the visible region, silica is proposed here whose threshold damage is a few orders of magnitude higher. Moreover, lower AFF and fewer air holes in the proposed ES-PCF design architecture would facilitate easy fabrication of this single material PCF by using the established sol-gel fabrication technique. Further investigation in this newly designed spiral cladding architecture will yield its suitability to other PCF related applications.

References

1. J. K. Ranka, R. S. Windeler, and A. J. Stentz, "Visible continuum generation in air silica microstructure optical fibers with anomalous dispersion at 800 nm," *Opt. Lett.* **25**(1), 25–27 (2000).
2. J. M. Dudley, G. Genty, and S. Coen, "Supercontinuum generation in photonic crystal fiber," *Rev. Mod. Phys.* **78**(4), 1135–1184 (2006).
3. A. Kudlinski, G. Bouwmans, M. Douay, M. Taki, and A. Mussot, "Dispersion-Engineered Photonic Crystal Fibers for CW-Pumped Supercontinuum Sources," *J. Lightwave Technol.* **27**(11), 1556–1564 (2009).
4. M. Liao, X. Yan, G. Qin, C. Chaudhari, T. Suzuki, and Y. Ohishi, "A highly non-linear tellurite microstructure fiber with multi-ring holes for supercontinuum generation," *Opt. Express* **17**(18), 15481–15490 (2009).
5. A. Agrawal, N. Kejalakshmy, J. Chen, B. M. A. Rahman, and K. T. V. Grattan, "Golden spiral photonic crystal fiber: polarization and dispersion properties," *Opt. Lett.* **33**(22), 2716–2718 (2008).
6. A. Agrawal, N. Kejalakshmy, J. Chen, B. M. A. Rahman, and K. T. V. Grattan, "Soft glass equiangular spiral photonic crystal fiber for supercontinuum generation," *IEEE Photon. Technol. Lett.* **21**(22), 1722–1724 (2009).
7. C. Seaton and J. Clowes, "Supercontinuum developments–research, exploitation and applications," *Opt. Photonics News* **20**(12), 19 (2009).
8. J. Cascante Vindas, S. Torres Peiró, and A. Diez M. V. Andrés, "Supercontinuum generation in highly Ge-doped core Y shaped microstructured optical fiber," *Appl. Phys. B* **98**(2–3), 371–376 (2009).
9. K. Mukasa, R. Miyabe, K. Imamura, and T. Yagi, "Hole-assisted fibers with λ_0 around 1000 nm and holey fibers with λ_0 around 500 nm," *J. Lightwave Technol.* **27**(11), 1716–1724 (2009).
10. R. T. Bise and D. Trevor, "Sol-gel derived microstructured fiber: fabrication and characterization," *Technical Digest of Optical Fiber Communication Conference (OFC/OSA 2005)*, Paper OWL6, Anaheim, California (2005).
11. COMSOL Multiphysics, version 3.2 (2005).
12. S. Roy, K. Mondal, and P. Roy Chaudhuri, "Modeling the tapering effects of fabricated photonic crystal fibers and tailoring birefringence, dispersion, and supercontinuum generation properties," *Appl. Opt.* **48**(31), G106–G113 (2009).